INDIAN JOURNAL OF SCIENCE AND TECHNOLOGY

RESEARCH ARTICLE

An Efficient Transform based Low Rank Tensor Completion to Extreme Visual Recovery

Sunil Kumar Jyothula[1,2]*, **Jaya Chandra Prasad Talari**[3]

1 Research scholar, Department of Electronics and Communication Engineering, JNTUA, Anantapur, Andhra Pradesh, India
2 Assistant Professor, Department of Electronics and Communication Engineering, Malla Reddy Engineering College, Secunderabad, Telangana, India
3 Professor, Department of Electronics and Communication Engineering, Rajeev Gandhi Memorial College of Engineering and Technology, Affiliated to JNTUA, Nandyal, Andhra Pradesh, India

OPEN ACCESS

Received: 31-01-2022
Accepted: 20-02-2022
Published: 09.04.2022

Citation: Jyothula SK, Talari JCP (2022) An Efficient Transform based Low Rank Tensor Completion to Extreme Visual Recovery. Indian Journal of Science and Technology 15(14): 608-618. https://doi.org/10.17485/IJST/v15i14.264

* **Corresponding author**.

jskumar457@gmail.com

Funding: None

Competing Interests: None

Published By Indian Society for Education and Environment (iSee)

ISSN
Print: 0974-6846
Electronic: 0974-5645

Abstract

Objective: To propose an optimization approach in recovering of the corrupted tensors in the high dimensional real time data. **Methods:** The recovering of corrupted tensors is performed by low-rank tensor completion methods. The tensor decomposition methods are used in tensor completion methods. These Tensor decomposition methods; candecomp / parafac (CP), tucker and higher-order Singular Value Decomposition (HoSVD) are used to minimize the rank of a tensor data. The limitations are in finding the rank of a tensor. **Findings:** The recovered data using the lifting transform induced tensor-Singular Value Decomposition (t-SVD) technique were assessed utilizing the Peak Signal to Noise Ratio (PSNR), Structural Similarity (SSIM), Naturalness Image Quality Evaluator (NIQE), and Perceptual Image Quality Evaluator (PIQE). When compared to state-of-the-art approaches, the low rank assumption condition with the lifting transform consideration gave good data recovery for every missing ratio. **Novelty:** The missing data is calculated by lifting polyphase structures by utilizing the available data. The polyphase structures are splitting the value into equivalent multiple triangular matrices, these are processed with the t-SVD to have the better approximation tensor rank.

Keywords: Tensor Completion; Transformbased Optimization; 5/3 Lifting Wavelet Transform; Lowrank tensor completion; tSVD

1 Introduction

Estimating the missing tensor observations from the limited uncorrupted tensor observations is very difficult [(1)]. To recover missing observations, repeated patterns present in the image may be used [(2)]. It is providing the solutions to wide range of problems in machine learning, computer vision, appearance acquisition, video coding, scan completion, subspace clustering, and compressed sensing applications [(3–6)]. The two-dimensional data completion difficulties are addressed with the nuclear norm approach; it replaces the rank function [(7)] and it is termed as Low Rank Minimization.

Singular value thresholding technique used to provide solutions to numerous Low-Rank optimization problems. It had poor recovery in the two-dimensional data because the all-singular values are minimized, it led to the loss of major structure information. The truncated nuclear norm regularization [8] minimizes singular values based on rank by performing the two-step process. The singular value shrinkage process is performed along with the optimization process. Identification of a rank for the two-dimensional is simple and computation costs are also low. If the missing ratio is increasing the recovering of the image becomes more difficult and less accurate. An introduction of a sparse regularizer can provide a better approximation. The sparse regularizer is framed with a two-step process [9]; firstly, a transform operator induced with singular value decomposition is used to find the missing data and update the data; and secondly, solves the constrained optimization function. This constrained optimization function is addressed by Alternating Direction Method of Multipliers (ADMM) framework. In the case of multidimensional data, finding the optimal rank (tensor rank) is a difficult task, because of the multidimensional algebraic properties.

Kilmer et al. [10] introduced the t-SVD approach; it is well performing in capturing the spatial-shifting correlation of high dimensional data. Let the three-dimensional data tensor be decomposed as two orthogonal tensors and one diagonal tensor as similar to two-dimensional SVD. The tensor completion algorithms High Accuracy Low Rank Tensor Completion (HaLRTC), Fast Low Rank Tensor Completion (FaLRTC) and Simple Low Rank Tensor Completion (SiLRTC) are introduced [6]. Further, to improve the recovery of high dimensional data, the truncated nuclear norm is extended to tensors and introduced with the Discrete Cosine Transformation (DCT) [11]. Here the inclusion of DCT provides piecewise similarity among the recovered tensors in the image. The unitary transform-based t-SVD approach was introduced to improve PSNR in hyperspectral images [12]. Here another transform-based t-SVD approach is presented to improve the visual quality of the highly corrupted high-dimensional data. The second-generation wavelet transform [13] features: the original data may be changed with its inverse transform without affecting the basic structural information; auxiliary memory is not needed to implement. It is also a reversible integer wavelet transform, easy to implement and understand.

A linked transform-based low-rank tensor representation that fully uses the redundancy in spatial and spectral / temporal dimensions and multi-scale spatial nature, resulting in an efficient multi low tensor rank approximation. They have used two spatial dimensions with the two-dimensional framelets, and for temporal /spectral dimension one / two-dimension Fourier transform is used, and a Karhunen - Loéve transform (by singular value decomposition) to the changed tensors [14]. Tensor Train rank reduction is conducted on a created higher-order tensor called group by stacking comparable cubes, which naturally and completely exploits Tensor Train rank's ability to create high-order tensors. To every group of Tensor Train, low-rankness is produced by perturbation analysis [15].

The residual texture information in a spectrum variation image is considered by spatial domain spectral residual total variation (SSRTV). SSRTV calculating a 2DTV for the residual image after evaluating the difference between the pixel values of neighboring bands. Low-rank Tucker decomposition takes advantage of hue, saturation, and intensity (HSI) worldwide, low-rankness and spatial–spectral correlation (LRTD). Furthermore, the $l_{2,1}$ norm was shown to be more effective in dealing the sparse noise, particularly sample-specific noise like stripes [16]. In the Tensor Ring (TR) decomposition methodology, the block Hankelization method is used to convert the corrupted tensor data into a 7-D higher order tensor. With rank, incremental and multistage methods, the higher order tensor is recovered by employing TR decomposition. Here the rank incremental approach is used to determine TR rankings [17].

The existing and proposed approaches were evaluated using the Full Reference Assessment metrics named PSNR and SSIM, and No-Reference Assessment metrics named NIQE [18], and PIQE [19]. The values obtained are superior to the existing approaches.

The main contributions of the work are

- The 5/3 wavelet filter-based lifting scheme induced t-SVD is proposed to recover the high dimensional data, when the data consists of more than 80 percent of corrupted observations.
- The visual quality of highly corrupted high-dimensional data under low tensor rank assumptions is improved.
- The PSNR and SSIM are calculated for the reported high when compared with the existing approaches. The NIQE and PIQE are very small, which indicates extreme visual recovery with local and global information.

1.1 Notations and Preliminaries

The notations used are: Lowercase characters, such as $'\mathscr{X}'$are used to represent the scalars. Lowercase boldface characters, such as $'\mathscr{X}'$ are used to represent vectors. Matrices are symbolized by capital characters, such as $'\mathscr{X}'$. The boldface uppercase scripting characters, such as $'\mathscr{X}'$ indicate the tensors. The i^{th} frontal, lateral and horizontal slices are represented as $\mathscr{X}(:,:$

$,i), \mathscr{X}(:,i,:)$ and $\mathscr{X}(i,:,:)$respectively. Eqn. (1) and (2) are the block circulant tensor and unfolded tensor [3~6].

$$bcirc(\bar{X}) \triangleq \begin{bmatrix} X^{(1)} & X^{(n3)} & \ldots & X^{(2)} \\ X^{(2)} & X^{(1)} & \ldots & X^{(3)} \\ . & . & \ldots & . \\ . & . & \ldots & . \\ . & . & \ldots & . \\ X^{(n3)} & X^{(n3-1)} & \ldots & X^{(1)} \end{bmatrix} \tag{1}$$

$$unfold(X) \triangleq \begin{bmatrix} X^{(1)} \\ X^{(2)} \\ . \\ . \\ . \\ X^{(n3)} \end{bmatrix} \tag{2}$$

The following properties and notations are used in the solving of the objective function.

Tensor Product [3~6] Let $\mathscr{X} \in \mathbb{R}^{n1\times n2\times n3}$ and $\mathscr{Y} \in \mathbb{R}^{n2\times n4\times n3}$ and . The tensor product between x and y can be written as

$$x * y = \text{ fold } (\text{bcirc}(x).\ \text{unfold } (y)) \tag{3}$$

Tensor Transpose [3~6] The transpose of a tensor $X \in R^{n1\times n2\times n3}$ becomes as X^T with order n2′n1′n3. The frontal slice needs to be transposed and then the order of the frontal slices from 2 to n3 are may be reversed.

$$\left(X^T\right)^{(1)} = \left(X^1\right)^{(T)}$$

$$\left(X^T\right)^{(i)} = \left(X^{n3-i+2}\right)^{(T)}, i = 2,3,\ldots,n3 \tag{4}$$

Identity Tensor [3~6] The identity tensor $X \in R^{n1\times n2\times n3}$ contains the first frontal slice $n \times n$ identity matrix, remaining frontal slices contains all zeros.

Orthogonal Tensor [3~6] A tensor $x \in \mathbb{R}^{n1\times n2\times n3}$ orthogonal if it satisfies

$$\mathscr{X}^T * \mathscr{X} = \mathscr{X} * \mathscr{X}^T = \mathfrak{I} \tag{5}$$

The Table 1 describes the notations with descriptions that are used.

2 5/3 Lifting induced t-SVD

The high-dimensional data processing requires huge storage, high data speeds for transmission, and accessing is difficult; to simplify the usage of storage and transmission data rates; the data will be compressed or encoded, during these processes, the tensor gets damaged. The corrupted tensors are less; the tensor can be recovered with conventional algorithms easily. If more tensors are corrupted the existing approaches are unable to recover. Here a transform-based optimization model is discussed to recover the tensors.

2.1 5/3 Lifting Wavelet Transform

The lifting wavelet transforms (LWT) play a vital role in image denoising, image compression, and image inpainting. The LWT features are: less computational complexity, fast, allows the one to custom design the filters, polyphase representation and allows in-place implementation. To build sparse approximations of most real time data, the LWT generated correlation structure may be used. The lifting structure begins with the well-known filters (h, g) and the filters are split into even and odd parts forming a polyphase matrix as

$$P(z) = \begin{bmatrix} h_e & g_e \\ h_o & g_o \end{bmatrix}$$

Table 1. Notation and Description

Notation	Description
$\|\|.\|\|_F$	Frobinous Norm
$\|\|.\|\|_2$	l_2-norm or m-norm
I	Corrupted high dimensional image
U, V	Unitary tensors obtained from tensor SVD
s_i	Prediction coefficients
t_i	Updation coefficients
$\widehat{X}$	Reconstructed matrix
$\widehat{I}$	Recovered tensor
$h,\ g$	Low pass and high pass filters
h_e, h_o	Even and Odd tensors obtained with low pass filter
g_e, g_o	Even and Odd tensors obtained with high pass filter
candecomp	Canonical Decomposition
parafac	Parallel Factorization

The polyphase matrix is factorized using the successive division method, which involves utilizing the Euclidean algorithm of the greatest common divisor (GCD) and selecting the proper Laurent polynomials. The factorization process aims to express the polyphase matrix as a series set of lower and upper triangular matrices. The first column of the polyphase matrix is factorized which results in the following matrix decomposition

$$\begin{bmatrix} h_e \\ h_o \end{bmatrix} = \prod_{i=1}^{n} \begin{bmatrix} q_i(z) & 1 \\ 1 & 0 \end{bmatrix} \begin{bmatrix} k \\ 0 \end{bmatrix}$$

k is the greatest common divisors and $q_i(z)$ is the quotient in the i^{th} step of the successive division approach of finding the greatest common-divisors.

Complementary polyphase filter g^0can be found where another polyphase matrix \widehat $\widehat{P}(z)$

$$\widehat{P}(z) = \begin{bmatrix} h_e(z) & \widehat{g_e}(z) \\ h_o(z) & \widehat{g_o}(z) \end{bmatrix} = \prod_{i=1}^{n} \begin{bmatrix} q_i(z) & 1 \\ 1 & 0 \end{bmatrix} \begin{bmatrix} k & 0 \\ 0 & 1/k \end{bmatrix}$$

The final polyphase factorization may be written as

$$\widehat{P}(z) == \prod_{i=1}^{n} \begin{bmatrix} 1 & s_i(z) \\ 0 & 1 \end{bmatrix} \begin{bmatrix} 1 & 0 \\ t_i(z) & 1 \end{bmatrix} \begin{bmatrix} k & 1 \\ 1 & 1/k \end{bmatrix}$$

k is the non-zero constant and $s_i(z)$ and $t_i(z)$ represents the dual lifting and primal lifting stages, respectively.

The analysis polyphase matrix gives the direct implementation of the forward transform of the lifting scheme. When compared to the standard wavelet approach, this reduces computing complexity. The better performance of the lifting scheme is dependent on the choice of the wavelet filter. Wavelet family has wide range of wavelet filters are available. The wavelet filter 'spl 53$'$ is the most familiar and lossless conversion filter. The $5/3$ wavelet is a biorthogonal wavelet with simple analysis and synthesis stages. It is able to calculate coefficients effectively with a smaller number of computations. The 5/3 filter-pair is made up of the 5 coefficients analysis low pass filter $'h'$, and the 3 coefficients analysis high-pass filter $'g'$. Figure 1 shows the lifting wavelet forward and reverse steps.

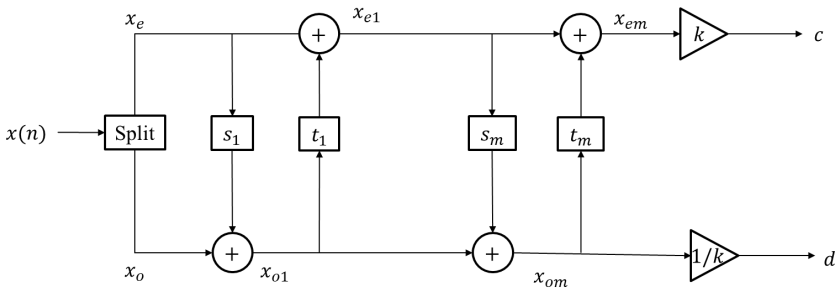

Fig 1. Lifting wavelet forward and reverse process

The tensor-SVD is performed to the lifting coefficients to obtain the sparse data in the corrupted data. Figure 2 shows the tensor-SVD process. Suppose $I \in C^{n_1 \times n_2 \times n_3}$ it can be factorized as $U \in C^{n_1 \times n_1 \times n_3}, V \in C^{n_2 \times n_2 \times n_3}$ *and* $S \in C^{n_1 \times n_2 \times n_3}$. Where the U, V, are the unitary tensors and S is the diagonal tensor consists of singular values of the high-dimensional data.

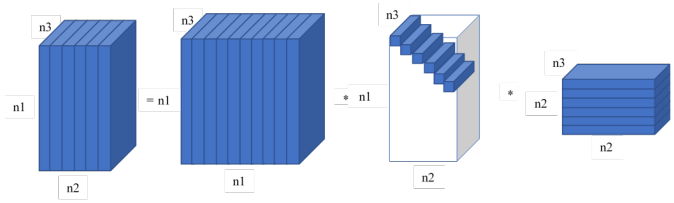

Fig 2. Tensor SVD of 3-dimensional data

The diagonal tensor will be reduced by using the truncation of uncorrelated singular values, it may be used the convex optimization, by utilizing W objective function can be reduced. The augmented Lagrange function becomes as eqn. (6)

$$\begin{aligned} \mathcal{J}_{k+1} &= arg\min_{\mathcal{J}} \| \mathcal{J} \|_* + \lambda \| \mathcal{W} \|_F \\ \mathcal{L}(\mathcal{J}, \mathcal{W}, \mathcal{Y}, \mu) &= \| \mathcal{J} \|_* - \mathrm{tr}\left(A_k * W * \mathcal{B}_k^T\right) + \langle y, \mathcal{J} - \mathcal{W} \rangle + \frac{\mu}{2} \| \mathcal{J} - W \|_F^2 \end{aligned} \tag{6}$$

Keep $\mathcal{W}_k$ and $\mathcal{Y}_k$ invariant $\mathcal{I}_{k+1}$ will be updated

$$J_{k+1} = \| \mathcal{J} \|_* + \langle \mathcal{Y}, \mathcal{J} - W \rangle + \frac{\mu}{2} \| \mathcal{J} - \mathcal{O} \|_F^2 \tag{7}$$

$$\mathcal{J}_{k+1} = \| \mathcal{J} \|_* + \frac{\mu}{2} \left\| J - \left(\mathcal{W}_k - \frac{1}{\mu} \mathcal{Y}_k \right) \right\|_F^2 \tag{8}$$

Based on the singular value thresholding shrinkage operation eqn. 9. can be solved easily.

By fixing the $\mathcal{I}_{k+1}$ and $\mathcal{Y}_k$ we solve $\mathcal{W}$

$$\begin{aligned} \mathcal{W}_{k+1} &= \arg\min_{\mathfrak{W}} \mathcal{L}(J_{k+1}, W_k, y_k) \\ &= \arg\min_{\mathfrak{W}} \frac{\mu}{2} \| J_{k+1} - W_k \|_F^2 - \mathrm{tr}\left(\left(\mathcal{A}_k * W * \mathcal{B}_k^T \right) + \langle y_k, J_{k+1} - \mathcal{W}_k \rangle \right) \end{aligned} \tag{9}$$

$$W_{k+1} = I_{k+1} + \frac{1}{\mu} \left(A_l^T * B_l + Y_k \right) \tag{10}$$

The update of $\mathcal{Y}_{k+1}$ is as eqn. 11

$$y_{k+1} = y_k + \mu \left(J_{k+1} - \mathcal{W}_{k+1} \right) \tag{11}$$

The proposed steps are framed as below

Algorithm: Lifting based t-SVD for Tensor Completion
Observation:
$\mathscr{I}$ is original incomplete data set, Ω represents the known elements, $\blacksquare_c$ indicates the unknown elements.
Initialization: $t = 1, \mathscr{Y} = \mathscr{J}, \mathrm{W} = \mathscr{J}, k = 1, \varepsilon, \mu = 5 \times 10^{-4}, l = 50$
given $\mathscr{J} \in \mathbb{R}^{m \times n \times p}$
Calculate the lifiting coefficnets to tensor $\mathscr{J}_k$
Approximations $'c'$ and details $'d'$ will be calculated using the 5/3 lifting wavelet filter
$[\mathscr{U}, \mathscr{S}, \mathscr{V}] = t - SVD(\mathscr{T}(\mathscr{J}_k))$ where $\mathscr{U}_k \varepsilon \mathbb{C}^{m \times m \times p}, \mathscr{V}_k \varepsilon \mathbb{C}^{n \times n \times p}, \mathscr{T}(\mathscr{J}_k)$ indicates the transform of data.
Compute $\mathscr{A}_l$ and $\mathscr{B}_l$ as follows $(r \leq \min\{m, n\})$
$\mathscr{A}_l = \mathscr{U}(::1:r;:)^T; \mathscr{B}_l = \mathscr{V}(::1:r;:)^T$
update $\mathscr{J}_{k+1}, \mathscr{W}_{k+1}, \mathscr{Y}_{k+1}, \mu$
Keep $\mathscr{W}_k$ and $y_k$invariant and update $\mathscr{J}_{\mathbf{k+l}}$from$L(\mathscr{J}, \mathscr{W}_k, y_k, \mu)$
By fixing $\mathscr{J}_{\mathbf{k+l}}$ and $y_k W$ may be calculated as
$\mathscr{W}_{\mathbf{k+l}} = \arg\min_{\mathscr{W}} \mathscr{L}(\mathscr{J}, \mathscr{W}_k, \mathscr{Y}_k, \mu)$
Update $\mathscr{Y}_{k+1}$ directly through
$\mathscr{Y}_{\mathbf{k+l}} = y_k + \mu(\mathscr{J}_{k+1} - \mathscr{W}_{k+1})$:
$k = k + 1$
Until $\|\mathscr{J}_{k+1} - \mathscr{J}_k\| \leq \varepsilon$ or $k > l$
Output: The Recovered Image $\hat{\mathcal{J}} = \mathscr{J}_{k+1}$

The 5/3 lifting wavelet inclusion in t-SVD, which is improving the effective calculation of missing tensors. The analysis filter coefficients are predicted by the odd location tensors by using the even location tensors. The even locations tensors are the approximation information it will have and the odd location tensors will have the details information of tensors. The odd location tensors may not be used in the prediction and updation of the odd location tensors. The missing or corrupted tensors will be updated with this process. The tensor SVD is applied to the retrieved tensors to minimize the rank of a tensor in the augmented lagrangian approach.

3 Results and Discussion

The proposed approach is tested with the various classes of images like natural images, and scenes, etc. The system configuration used for the work is Intel i5 8th generation processor with 8GB RAM, MATLAB 2019a. The images used for experimentation are of size 256⊠256 and they are listed in Figure 3.

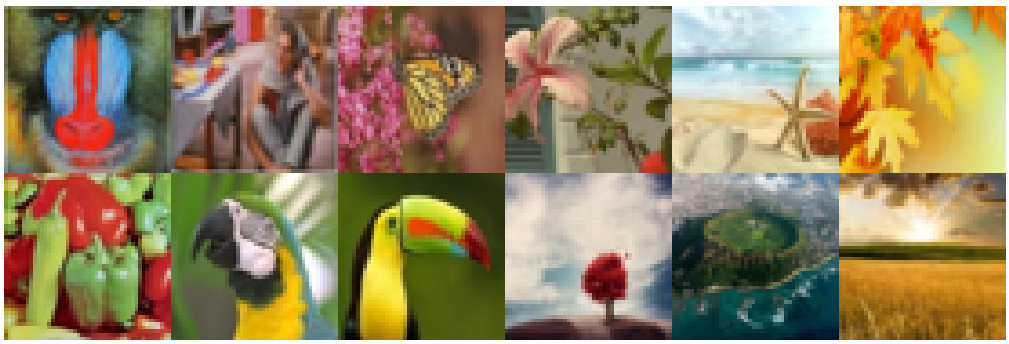

Fig 3. Sample High-dimensionaldata set

The color images are degraded by 10% to 90% random pepper noise to make the intensity values to zero. The 5/3 wavelet with decomposition and reconstruction level is 2. The tensor rank 'r' is considered to be from 1 to 10. The optimal values are achieved at rank 3. The $\varepsilon = 10^{-3}$, ρ=1.05, l = 50, and $\mu = 5 \times 10^{-4}$ to balance the efficiency and the accuracy of our approach. The FRIQA metrics PSNR and SSIM are used to evaluate the approaches. The PSNR is evaluated as

$$psnr = 10log_{10}\frac{(maximum\ value\ in\ the\ tensor\ elements)^2}{MSE^2} \qquad (12) \qquad (12)$$

where –

The SSIM is evaluated with the luminance distortion, contrast distortion and loss of correlation.

$$ssim = l(I,R)\,c(I,R)\,s(I,R)$$

Where $l(I,R) = \frac{2\mu_I\mu_R+C_1}{\mu_I^2+\mu_R^2+C_1}$, $c(I,R) = \frac{2\sigma_I\sigma_R+C_2}{\sigma_I^2+\sigma_R^2+C_2}$ and $s(I,R) = \frac{2\sigma_{IR}+C_3}{\sigma_I\sigma_R+C_3}$

Here $\mu_I$and μ_R are indicates the mean values of the reference and recovered data. $\sigma_I$and $\sigma_R$are indicates the standard deviation of the reference and recovered data. C_1, $C_2$and C_3 are the positive constants to avoid null denominator.

Table 2. Comparison of PSNR (in dB) of recovered images by the proposed and existing methods

Image	TNNR [8]	LRTF [5]	Lifting based t-SVD (Proposed)
	24.29	26.91	32.53
	17.93	20.57	29.54
	19.96	22.39	31.38

Table 2 represents the comparison of PSNR values in existing and the proposed methods recovered images from 85% missing observations.Here PSNR alone is not considered concluding which gives better performance. The SSIM, NIQE, and PIQE also considered they provided remarkably good results.

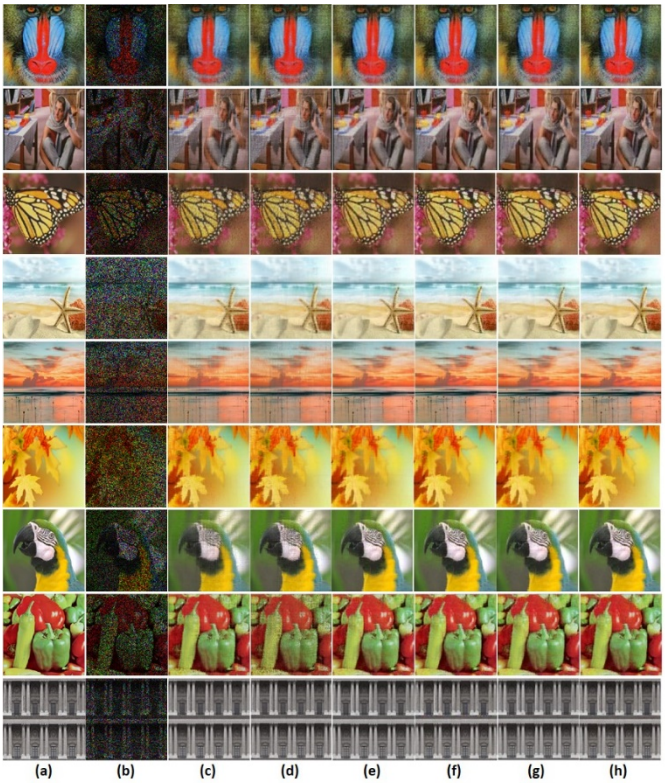

Fig 4. Recovered image results at 70% missing ratio with existing and proposed images. (a) Reference Image, (b) 70% of data randomly corrupted, (c) FaLRTC (Existing), (d) HaLRTC (Existing), (e) T-TNN with APGL(Existing), (f) T-TNN with APGL(Existing) (g) LRTM with APGL(Proposed), and (h) LRTM with ADMM (Proposed)

In Figure 4, Figure 5, and Figure 6 show the recovered images with the existing and proposed approaches, from the 70%, 80%, and 90% corrupted images, respectively. Fig 4 (i), and (ii) shows the reference image and 70% of the corrupted data in the image. In Figure 4 c-h show the existing and proposed approaches recovered images. The proposed approach recovered images have high visual clarity, when compared to existing approaches recovered images. Similarly, and Figure 5 and Figure 6 show that, the corrupted ratio is increased further by 80% and 90% the proposed approach is able to recover with good visual quality.

Fig 5. Recovered image results at 80% missing ratio with existing and prposed images. (a) Reference Image, (b) 80% of data randomly corrupted, (c) FaLRTC (Existing), (d) HaLRTC (Existing), (e) T-TNN with APGL (Existing), (f) T-TNN with APGL (Existing) (g) LRTM with APGL (Proposed), and (h) LRTM with ADMM (Proposed)

The performance evaluation parameters are stated in Figure 7 and Figure 8. The missing ratio to 10% to 90% the PSNR, SSIM, NIQE and PIQE are plotted for various images. Two image results are presented.

Figure 7 shows the PSNR, SSIM, NIQE, and PIQE measures of recovered pepper color image from 10 percent to 90 percent corrupted observations. The existing and proposed approaches have almost similar PSNR values, but the SSIM values are different. The proposed approach has superior values than existing approaches. The NRIQA metrics NIQE and PIQE results are very minimal values are obtained, which is conveying that the proposed approach is better than existing approaches. The PIQE values of recovered data are fluctuating when the missing ratio is small, to those recovered data also given high values, but image quality is good. These differences are identified with existing algorithms also.

Figure 8 presents the FRIQA and NRIQA evaluation metrics for recovered results of high-dimensional data (color image). The missing ratio vs PSNR of the recovered scene image at different missing ratios. To these images set of high-dimensional data achieved small improvement in the PSNR values, with proposed approach and the SSIM values are high at the high missing ratios with the proposed approach. The NIQE and PIQE to different missing ratios of recovered scene image. Figure 9 shows FRIQA and NRIQA metrics with different missing ratios, with different ranks. At small ranks, the PSNR values are good at high missing ratios and the SSIM with different ranks and different missing ratios, at low ranks; thee SSIM values are high at high missing ratios. With the smaller rank, the recovered pepper image at 80% missing ratio is attained as 0.8918 with tensor rank 5.

Similarly, the PSNR achieved as 31.62dB to the same missing ratio and rank. The NIQE is describes the naturalness in the recovered image, while calculating the NIQE score, reference image is not considered. The value is attained as 9.4 to the recovered image at 80% missing ratio with rank 5. Minimum values always indicate the good recovery of the image. Another NRIQA metric is used to evaluate the recovered data i.e., PIQE. The PIQE is also not required to have any reference to evaluate and the value is 27.33. The proposed approach has got the minimum values compared with existing approaches.

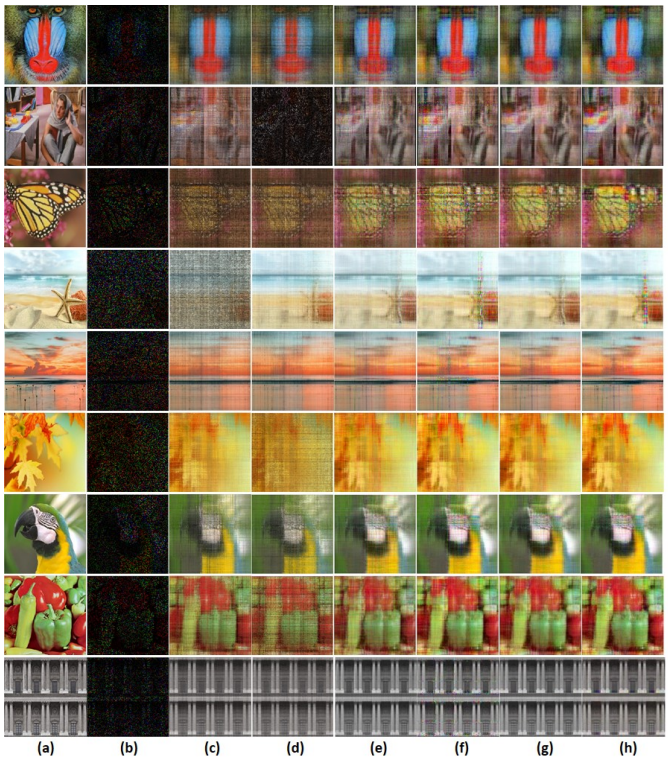

Fig 6. Recovered image results at 90% missing ratio with existing and proposed images. (a) Reference Image, (b) 90% of data randomly corrupted, (c) FaLRTC (Existing), (d) HaLRTC (Existing), (e) T-TNN with APGL (Existing), (f) T-TNN with APGL (Existing), (g) LRTM with APGL (Proposed), and (h) LRTM with ADMM (Proposed)

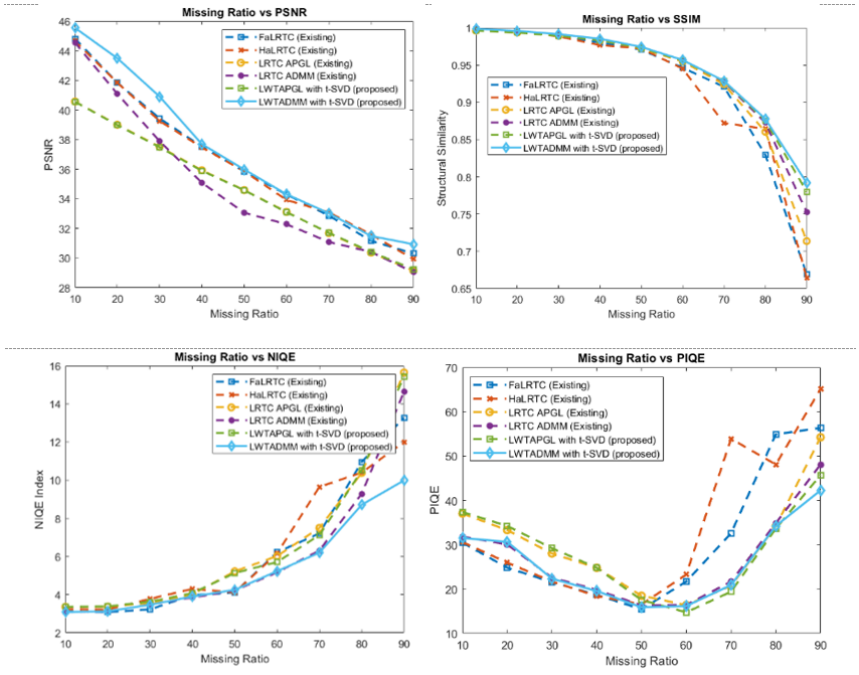

Fig 7. Performance evaluationmetrics for the recovered pepper image at various missing ratios

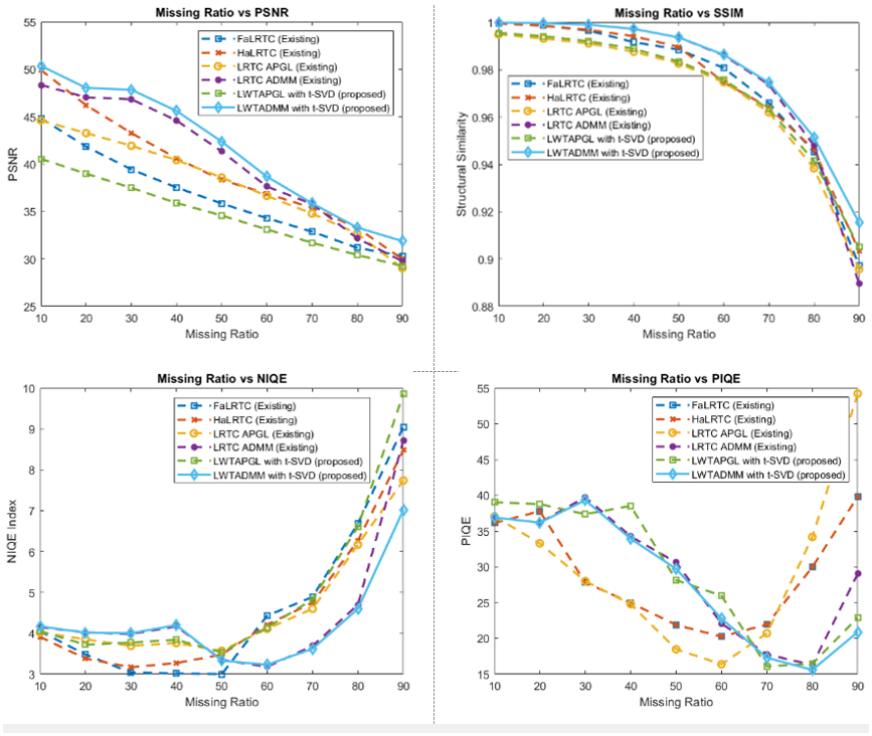

Fig 8. Performance evaluationmetrics for the recovered scene image at various missing ratios

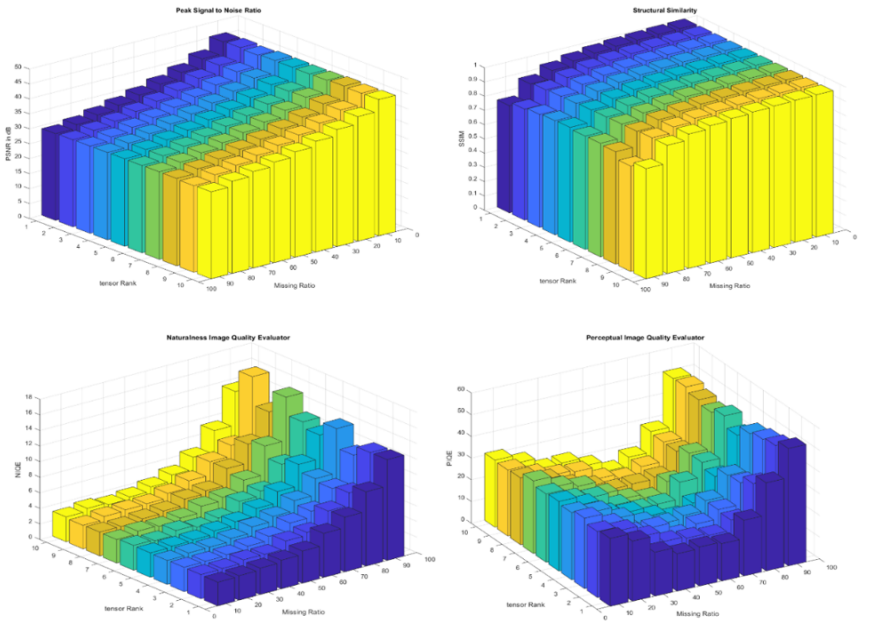

Fig 9. Performance metrics withvarious ranks and with different missing ratios

4 Conclusions

The proposed approach is able to recover the high dimensional data from very less observations efficiently. The lifting wavelets features in-place and custom design of filters are made the design simple, fast and accurate with tensor low rank assumptions. The t-SVD helps in finding the minimum tensor rank. The proposed approach is evaluated with the FRIQA and NRIQA measures along existing methods. The PSNR and SSIM recorded as high values 31.62dB and 0.8918 respectively to recovered image at 80% corrupted observations. The NRIQA measures NIQE and PIQE values are reported as minimum values (9.4 and 27.33 respectively) at highly corrupted ratios. The missing ratio is increasing, the recovery is consistent in proposed approach compared with the state-of-the-art methods.

References

1) Xue S, Qiu W, Liu F, Jin X. Low-Rank Tensor Completion by Truncated Nuclear Norm Regularization. *2018 24th International Conference on Pattern Recognition (ICPR)*. 2018;p. 2600–2605. doi:10.1109/ICPR.2018.8546008.
2) Su Y, Wu X, Liu W. Low-Rank Tensor Completion by Sum of Tensor Nuclear Norm Minimization. *IEEE Access*. 2019;7:134943–134953. Available from: https://dx.doi.org/10.1109/access.2019.2940664.
3) Zhang L, Song L, Du B, Zhang Y. Nonlocal Low-Rank Tensor Completion for Visual Data. *IEEE Transactions on Cybernetics*. 2021;51(2):673–685. Available from: https://dx.doi.org/10.1109/tcyb.2019.2910151.
4) Huang H, Liu Y, Liu J, Zhu C. Provable tensor ring completion. *Signal Processing*. 2020;171:107486–107486. Available from: https://dx.doi.org/10.1016/j.sigpro.2020.107486.
5) Chen L, Jiang X, Liu X, Zhou Z. Logarithmic Norm Regularized Low-Rank Factorization for Matrix and Tensor Completion. *IEEE Transactions on Image Processing*. 2021;30:3434–3449. Available from: https://dx.doi.org/10.1109/tip.2021.3061908.
6) Liu J, Musialski P, Wonka P, Ye J. Tensor Completion for Estimating Missing Values in Visual Data. *IEEE Transactions on Pattern Analysis and Machine Intelligence*. 2013;35(1):208–220. Available from: https://dx.doi.org/10.1109/tpami.2012.39.
7) Recht B, Fazel M, Parrilo PA. Guaranteed Minimum-Rank Solutions of Linear Matrix Equations via Nuclear Norm Minimization. *SIAM Review*. 2010;52(3):471–501. Available from: https://dx.doi.org/10.1137/070697835.
8) Hu Y, Zhang D, Ye J, Li X, He X. Fast and Accurate Matrix Completion via Truncated Nuclear Norm Regularization. *IEEE Transactions on Pattern Analysis and Machine Intelligence*. 2013;35(9):2117–2130. Available from: https://dx.doi.org/10.1109/tpami.2012.271.
9) Dong J, Xue Z, Guan J, Han ZF, Wang W. Low rank matrix completion using truncated nuclear norm and sparse regularizer. *Signal Processing: Image Communication*. 2018;68:76–87. Available from: https://dx.doi.org/10.1016/j.image.2018.06.007.
10) Kilmer ME, Martin CD. Factorization strategies for third-order tensors. *Linear Algebra and its Applications*. 2011;435(3):641–658. Available from: https://dx.doi.org/10.1016/j.laa.2010.09.020.
11) Han ZF, Leung CS, Huang LT, So HC. Sparse and Truncated Nuclear Norm Based Tensor Completion. *Neural Processing Letters*. 2017;45(3):729–743. Available from: https://dx.doi.org/10.1007/s11063-016-9503-4.
12) Song G, Ng MK, Zhang X. Robust tensor completion using transformed tensor singular value decomposition. *Numerical Linear Algebra with Applications*. 2020;27(3). Available from: https://dx.doi.org/10.1002/nla.2299.
13) Ganesan T, Rajarajeswari P, Nayak SR, Bhatia AS. A novel genetic algorithm with CDF5/3 filter-based lifting scheme for optimal sensor placement. *International Journal of Innovative Computing and Applications*. 2021;12(2/3):67–67. doi:10.1504/IJICA.2021.113746.
14) Wang JL, Huang TZ, Zhao XL, Jiang TX, Ng MK. Multi-Dimensional Visual Data Completion via Low-Rank Tensor Representation Under Coupled Transform. *IEEE Transactions on Image Processing*. 2021;30:3581–3596. Available from: https://dx.doi.org/10.1109/tip.2021.3062995.
15) Ding M, Huang TZ, Zhao XL, Ng MK, Ma TH. Tensor train rank minimization with nonlocal self-similarity for tensor completion. *Inverse Problems & Imaging*. 2021;15(3):475–475. Available from: https://dx.doi.org/10.3934/ipi.2021001.
16) Kong X, Zhao Y, Chan JCW, Xue J. Hyperspectral Image Restoration via Spatial-Spectral Residual Total Variation Regularized Low-Rank Tensor Decomposition. *Remote Sensing*. 2022;14(3):511–511. Available from: https://dx.doi.org/10.3390/rs14030511.
17) Farnaz S, Andrzej C. Image Completion in Embedded Space Using Multistage Tensor Ring Decomposition. 2021;4. Available from: https://doi.org/10.3389/frai.2021.687176.
18) Mittal A, Soundararajan R, Bovik AC. Making a "Completely Blind" Image Quality Analyzer. *IEEE Signal Processing Letters*. 2013;20(3):209–212. Available from: https://dx.doi.org/10.1109/lsp.2012.2227726.
19) Venkatanath N, Praneeth D, Chandrasekhar BM, Channappayya SS, Medasani SS. Blind image quality evaluation using perception based features. *2015 Twenty First National Conference on Communications (NCC)*. 2015;p. 1–6. doi:10.1109/NCC.2015.7084843.